Journal of King Saud University - Science 36 (2024) 103302

HOSTED BY

Contents lists available at ScienceDirect

Journal of King Saud University - Science

journal homepage: www.sciencedirect.com

Full Length Article

Synthesis, Jahn-Teller labeled *via* crystal structure in *trans*-$(ClO_4)_2Cu^{II}(Me_2N\text{-}Py)_4$ complex: S9/S6/C-H…O synthons, thermal, physicochemical and 1BNA-docking

A. AlAli [a,1], A. AlObaid [b,1], B.S. Chethan [c], K. Shalalin [d], N. Alzeqri [b], K. Alkanad [e], N.K. Lokanath [e], A. Zarrouk [f], I. Warad [g,*], S.A. Khanum [a,*]

[a] Department of Chemistry, Yuvaraja's College, University of Mysore, Mysuru 570 005, Karnataka, India
[b] Department of Chemistry, College of Science, King Saud University, P.O. Box 2455, Riyadh 11451, Saudi Arabia
[c] Department of Basic Science, Amrita Institute of Engineering and Management Sciences, Bidadi, Bengaluru 572109, India
[d] Department of Dentistry and Dental Surgery, Faculty of Medicine and Health Sciences, An-Najah National University, P.O. Box 7, Nablus, Palestine
[e] Department of Studies in Physics, University of Mysore, Manasagangotri, Mysuru 570 006, India
[f] Laboratory of Materials, Nanotechnology, and Environment, Faculty of Sciences, Mohammed V University in Rabat, P.O. Box. 1014, Agdal-Rabat, Morocco
[g] Department of Chemistry, AN-Najah National University, P.O. Box 7, Nablus, Palestine

ARTICLE INFO

Keywords:
$[Cu(Py)_4]$
XRD/HSA
Docking
Jahn-Teller
Thermal

ABSTRACT

The synthesis of the *trans*-$(ClO_4)_2Cu^{II}(Me_2N\text{-}Py)_4$ complex (where Me_2N-Py = N,N-dimethylpyridin-4-amine ligand) in significant yield involved the reaction of excess Me_2N-Py ligand with $Cu(ClO_4)_2{\cdot}6H_2O$ in MeOH solvent. The progression of the complex synthesis was monitored by UV–Vis, FT-IR, EDX, XRD, MS, SEM, CHN-EA, and TG/DTG. The resulting complex crystallized in the Triclinic space $P\bar{1}$. In the solid state, the desired complex structure discrete a neutral *trans*-$(ClO_4)_2Cu^{II}(Me_2N\text{-}Py)_4$ formula, with copper(II) adopting a distorted octahedral environment formed by four Me_2N-Py ligands occupying the square planar position $Cu(Py)_4$, meanwhile, the two ClO_4 are in linear *trans*-position. The XRD measurements proved the existence of elongation Jahn-Teller distortion in the synthesized complex. Furthermore, a comprehensive analysis of the desired complex, including. XRD/HSA interactions revealed the presence of two S9 and S6 main 2D-synthons primarily formed through C_{ph}.H….O_{ClO3} and C_{Me}.H…O_{ClO3} non-classical H-bonding interactions. Thermal stability assessments through TG/DTG indicated that the complexes with the most stable behavior underwent two degradation steps. The molecular docking of the desired complex against 1BNA-DNA was also evaluated.

1. Introduction

Several inorganic chemists have designed octahedral copper(II) complexes using monodentate ligands obtained from pyridine derivatives (Santana et al., 2020; Masternak et al., 2021; Patel et al., 2010; Handy et al., 2017; Warad et al., 2018; Nnabuike et al., 2023). The redox characteristics of Cu(II) complexes have been thoroughly evaluated because of their biological relevance to imitateprotein functions (Fathy et al., 2022; Adhikari et al., 2022; Graur et al., 2023; Alem et al., 2023; Fathima et al., 2020; Andrejević et al., 2023; Jiang et al., 2007; Czaikowski et al., 2022; Balakrishnan et al., 2017; Fu et al., 2015; Jevtovic et al., 2023; Puchoňová et al., 2017; Anupama et al., 2017). [Copper(II)/Py]/[Copper(II)/phen] and their derivative complexes are of great importance among these complexes because of their flexibility to alter structurally and their wide range as DNA-binding, antibacterial, and COX/LOX-inflammation (AlAli et al., 2023; AlAli et al., 2023; Zabiulla et al., 2023; Begum et al., 2014). Supramolecular interactions, such as π-π stacking and hydrogen bonding, are essential in crystal engineering as they enable precise molecular recognition and facilitate the self-assembly of distinct supramolecular synthons (Balakrishnan et al., 2017). Octahedral Cu(II) complexes with d^9 centres are commonly recognized to have the ability to display a Jahn-Teller distortion. This distortion is made possible by the existence of unpaired electrons located in the d-orbital. In the theorem of Jahn–Teller, the degeneracy in the orbitals (d-orbitals spin-splitting) results in a simultaneous compression or elongation along one Z-axis as in Scheme 1, which

* Corresponding authors.
E-mail addresses: warad@najah.edu (I. Warad), shaukathara@yahoo.co.in (S.A. Khanum).
[1] A. AlAli and A. AlObaid contributed equally to this work.

https://doi.org/10.1016/j.jksus.2024.103302
Received 4 March 2024; Received in revised form 9 June 2024; Accepted 10 June 2024
Available online 16 June 2024

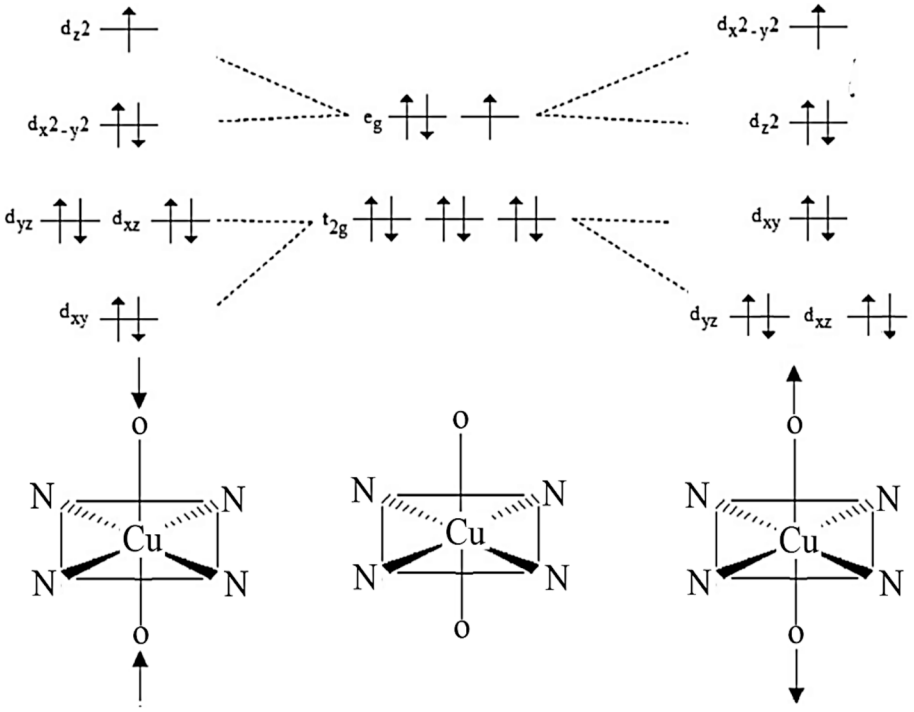

Scheme 1. The elongation/compression Jahn–Teller diagram in *the trans*-O_2CuN_4 complex.

Table 1
Trans-$(ClO_4)_2Cu^{II}(Me_2N\text{-}Py)_4$ crystal data.

Empirical formula	$C_{28}H_{40}Cl_2CuN_8O_8$
Formula weight	751.12
Temperature (K)	293
Wavelength	0.71073
Crystal system, Space group, Z	Triclinic, *P*1, 4
a/*b*/*c* (Å)	11.059(4)/16.743(6)/20.251(7)
α/β/γ (°)	97.360(5)/104.087(16)/102.733(8)
Volume (Å^3)	3481(2)
ρ_{calc}, Mg/cm^3	1.433
Absorption coefficient (μ/mm^{-1})	0.839
F(000)	1564
2θ range for data collection (°)	3.10 to 23.00
Index ranges	$-12 \le h \le 10$, $-18 \le k \le 18$, $-22 \le l \le 22$
Reflections collected	13,810
Independent reflections	9589
Refinement method	Full matrix least-squares on F^2
Absorption correction	Semi-empirical from equivalents
Data/restraints/parameters	9589/120/955
Goodness-of-fit on F^2	1.05
Final R indexes [I > 2σ (I)]	$R1 = 0.0756$, $wR2 = 0.1883$
Final R indexes [all data]	$R1 = 0.1215$, $wR2 = 0.2286$
Largest diff. Peak/hole (eÅ^{-3})	0.547 and −0.616

depicts the resultant *trans*-O_2CuN_4 complex electrical configuration. It is common practice to investigate these complexes' structures and any Jahn-Teller effect distortions using experimental methods including X-ray crystallography and spectroscopy.

Molecular docking is a powerful tool for understanding the interaction between organic/inorganic material and DNA or enzymes. By utilizing non-covalent interactions, several studies offer vital insights into the mechanism of action by inserting a molecule at the binding site of a specific area on DNA or enzyme (Warad et al., 2017). The utilization of in silico computational docking methods is crucial in the development of novel inorganic chemotherapeutic complexes that mimic the cisplatin drug. In silico docking analysis of various structural complexes enabled the exploration of energy, hydrogen bonding, and hydrophobic interactions, assisting in developing chemical therapies or understanding the behaviours of proposed drugs before they are introduced into biological cells.

This study details the synthesis of the *trans*-$(ClO_4)_2Cu^{II}(Me_2N\text{-}Py)_4$ complex utilizing 4-dimethylaminopyridine ligands. An XRD analysis was performed to confirm the presence of the distorted octahedral elongated Jahn-Teller complex. The HSA-compoution and exp. XRD reflected the excistence of 1 and 2D-synthons stabilized mainly by C-H…OCl H-bonds. In addition, various physicochemical and thermal analyses were employed to demonstrate the intricate structure. Subsequently, the complex was assessed using in silico molecular docking utilizing 1BNA-DNA.

2. Experimental analysis

2.1. Chemical and physical analyses

The Elementar Varrio EL analyzer was employed solely for comprehensive CHN microanalysis. The acquisition of the FT-IR spectra involved the utilization of a spectrophotometer manufactured by 621-Perkin-Elmer. The UV–Vis spectra measurements are obtained using a spectrophotometer manufactured by 4060-LKB-Biochrom. The MS analysis was performed with a ThermoScientific-TM TSQ-Altis-TM Triple Quadrupole Mass Spectrometer. Sigma–Aldrich provided the necessary quantity of solvents and compounds and TG analysis were recorded via TGA-7 PerkinElmer.

2.2. Preparation of trans-$(ClO_4)_2Cu^{II}(Me_2N\text{-}Py)_4$

0.5 g (1.34 mmol) of $Cu(ClO_4)_2{\cdot}6H_2O$ were dissolved in 30 ml of EtOH, and then 4 equivalents of N,N-dimethylpyridin-4-amine were added to the mixture. The reaction was performed in a closed system and stirred for 60 min until the blue colour transitioned into a greenish-blue. Subsequently, the reaction mixture was evacuated to a final volume of ~2 ml, and 40 ml of diethyl ether was added to cause the desired complex to precipitate. Following filtration, the resultant complex was extensively rinsed with 40 ml of CH_2Cl_2, yielding 83 %.

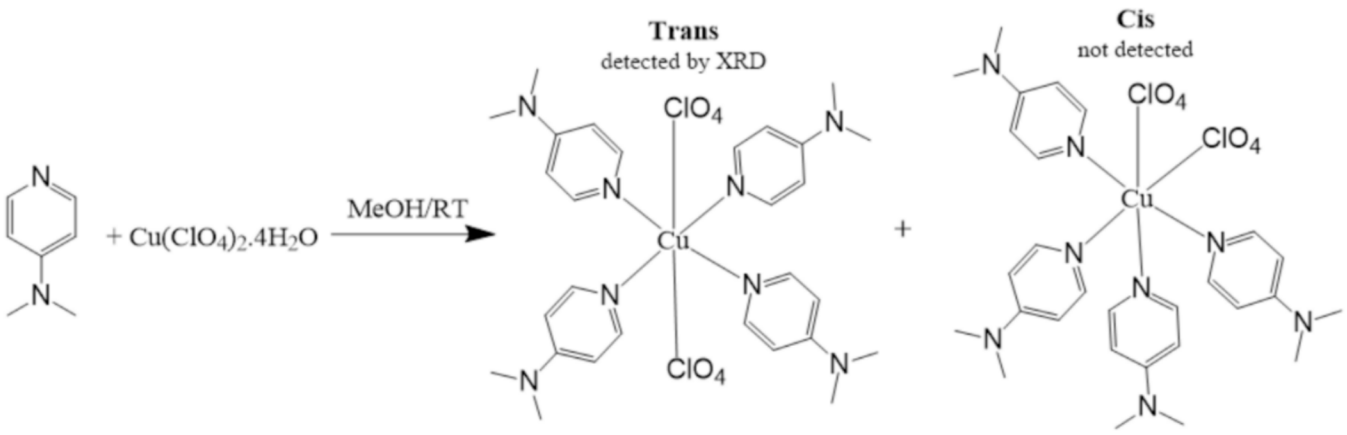

Scheme 2. Synthesis of *trans*-$(ClO_4)_2Cu^{II}(Me_2N\text{-}Py)_4$.

2.2.1. *Trans-$(ClO_4)_2Cu^{II}(Me_2N\text{-}Py)_4$*

MS *m/z* 751.2 [M^+] (theo. 752.4), m.p. = 308.5 °C, molecular formula $C_{28}H_{40}Cl_2CuN_8O_8$ Cal: C, 44.77; H, 5.37; and N, 14.92 %. Found C, 44.51; H, 5.22; N, 14.87 %, IR (νcm^{-1}): 3052 ($\nu_{C\text{-}H}$ of py), 2960–2840($\nu_{C\text{-}H}$ of Me), 1555 ($\nu_{N=C}$), 510–680 ($\nu_{Cu\text{-}N}$) and ($\nu_{Cu\text{-}O}$), and 1092 (ν_{ClO4}), UV–Vis in MeOH: λ_{max} ($\varepsilon/M^{-1}cm^{-1}$): 277 nm ($1.2 \times 10^4$) and 698 nm ($8.2 \times 10^2$).

2.3. HSA and XRD determinations

The HSA study was conducted utilizing CrystalExplorer 17.1 (Warad et al., 2017). The X-ray intensity data collection of the synthesized copper metal complex was conducted using graphite monochromatized Mo-Kα radiation (λ = 0.7107 Å). The complex's structure is determined using the intrinsic phasing approach, namely the SHELXT (Wolff et al., 2007). The refining process is carried out in Olex2 using SHELXL-2015, utilizing least-squares minimization against F2 (Sheldrick, 2008). The non-hydrogen atoms were identified in the structures using different Fourier maps, and their anisotropic thermal characteristics were revised. The hydrogen atoms were immobilized in a fixed geometric arrangement and refined using the riding model. The maximum positive value of the complex number in the final Fourier difference map is 0.547 $eÅ^{-3}$. The crystallographic data and the refinement details are provided in Table 1.

3. Results and discussion

3.1. Synthesis and analysis of trans-$(ClO_4)_2Cu^{II}(Me_2N\text{-}Py)_4$ complex

Trans-$(ClO_4)_2Cu^{II}(Me_2N\text{-}Py)_4$ complex was made available in high yields *via* treating of $Cu(ClO_4)_2{\cdot}6H_2O$ with 4xMe_2N-Py ligand in alcoholic medium at RT condition as seen in Scheme 2. The *cis*-$(ClO_4)_2Cu^{II}(Me_2N\text{-}Py)_4$ possible isomer was not detected, possibly because to its lower stability caused by steric hindrance, resulting in considerable internal repulsion compared to the *trans*-isomer. Under RT stirred condition, the reaction processed smoothly since the mixture colour was changed from light blue to green bluish within one hour, resulting in the formation of the desired complex. In the solid state, the *trans*-$(ClO_4)_2Cu^{II}(Me_2N\text{-}Py)_4$ complex was found to has a high melting point, blue in colour, and stable in an O_2-open atmosphere. Furthermore, its structure was proved *via* SEM, CHN-EA, UV–Vis, TG/DTG, GC–MS, EDX, FT-IR, and XRD-crystal.

The GCMS of the desired complex showed an excellent weak peak at *m/z* 751.2 (theoretical 752.4) supporting the formula weight of $[Cu^{II}(Me_2N\text{-}Py)_4(ClO_4)_2]^+$ complex, peak at *m/z* 652.2 can be attributed to one ClO_4 anion losing to form the mono-cation $[Cu^{II}(Me_2N\text{-}Py)_4ClO_4]^+$ stable fragment complex, losing of another ClO_4 to form the di-cation $[Cu^{II}(Me_2N\text{-}Py)_4]^{++}$ fragment complex can be cited to 552.2 *m/z* peak (Fig. 1a). The atomic composition of the desired complex has been confirmed via EDX reflected the appearance of O, N, C, Cu and Cl atoms only indicating the purity of the crystal structure (Fig. 1b). Moreover, the crystallinity and morphology were exterminated by SEM reflecting block particles as high crystalline rod-like morphology and complex purity (Fig. 1c). Nevertheless, SEM reflected a high crystalline structure and free of any irregularity, agglomeration, defect, and high particle stability had been recorded (Fig. 1c).

In solid-state FT-IR (Fig. 2a), the appearance of the stretching vibration strong band at 1092 cm^{-1} confirmed the existence of ClO_4 anion ligands in the complex backbone; moreover, the band at 3052 $\nu_{(Cph\text{-}H)}$, and 2960–2840 $\nu_{(CMe\text{-}H)}$ corresponded to Me_2N-Py ligands coordination. Additionally, peaks at 510–680 cm^{-1} $\nu_{(Cu\text{-}N)}/\nu_{(Cu\text{-}O)}$ supported the formation of Cu–N and Cu–O new bonds *via* L/M complexation process (Zeisel et al., 2019; Haynes et al., 1987; Spodine et al., 1993; Kongchoo et al., 2016). On the other hand, the UV–Vis behavior in MeOH reflected the *trans*-$(ClO_4)_2Cu^{II}(Me_2N\text{-}Py)_4$ complex with two absorption broadbands (Fig. 2b), one in the UV area with λ_{max} = 277 nm ($\varepsilon = 1.2 \times 10^4$ $M^{-1}cm^{-1}$) attributed to π-to-π e-transition and band in the visible region with λ_{max} 698 nm ($\varepsilon = 8.2 \times 10^2$ $M^{-1}cm^{-1}$) attributed to d-to-d e-transition. The presence of such visible signal corresponded to the blue color of the solution, confirming the occurrence of N-centers of Me_2N-Py bonding to the Cu(II) center.

3.2. XRD of the trans-$(ClO_4)_2Cu^{II}(Me_2N\text{-}Py)$ complex

The crystal and molecular structure of *trans*-$(ClO_4)_2Cu^{II}(Me_2N\text{-}Py)_4$ are depicted in Fig. 3a and Table 2, which contains selective angles and bond lengths. The Cu(II) ion in the desired complex adopts an elongated octahedral (Oh) geometry (Zeisel et al., 2019; Haynes et al., 1987; Spodine et al., 1993; Kongchoo et al., 2016), with six ligands coordinating it in a centrosymmetric manner (Fig. 3b). This structure consists of four Me_2N-Py ligands with Cu–N bond lengths of Cu1-N1 = 2.000(6) Å, Cu1-N4 = 2.003(7) Å, Cu1-N5 = 1.994(6) Å, Cu1-N6 = 2.011(6) Å, Cu2-N10 = 2.011(6) Å, Cu2-N11 = 2.009(5) Å, Cu2-N12 = 2.664(11) Å and Cu2-N13 = 2.007(5) Å on the square planar. Additionally, there are two perchlorates positioned along the long z-axis, with a Cu–O bond length of Cu1-O1 = 2.676 (6) Å, Cu1-O15A = 2.73 (3) Å, Cu2-O14 = 2.733(6) Å and Cu2-O5B = 2.73(3) Å. The XRD analysis revealed that the Cu–O bond length around the Cu(II) central atom increased by 8 % compared to similar systems (Kongchoo et al., 2016; Warad et al., 2019). This provided evidence for the occurrence of the widely recognized

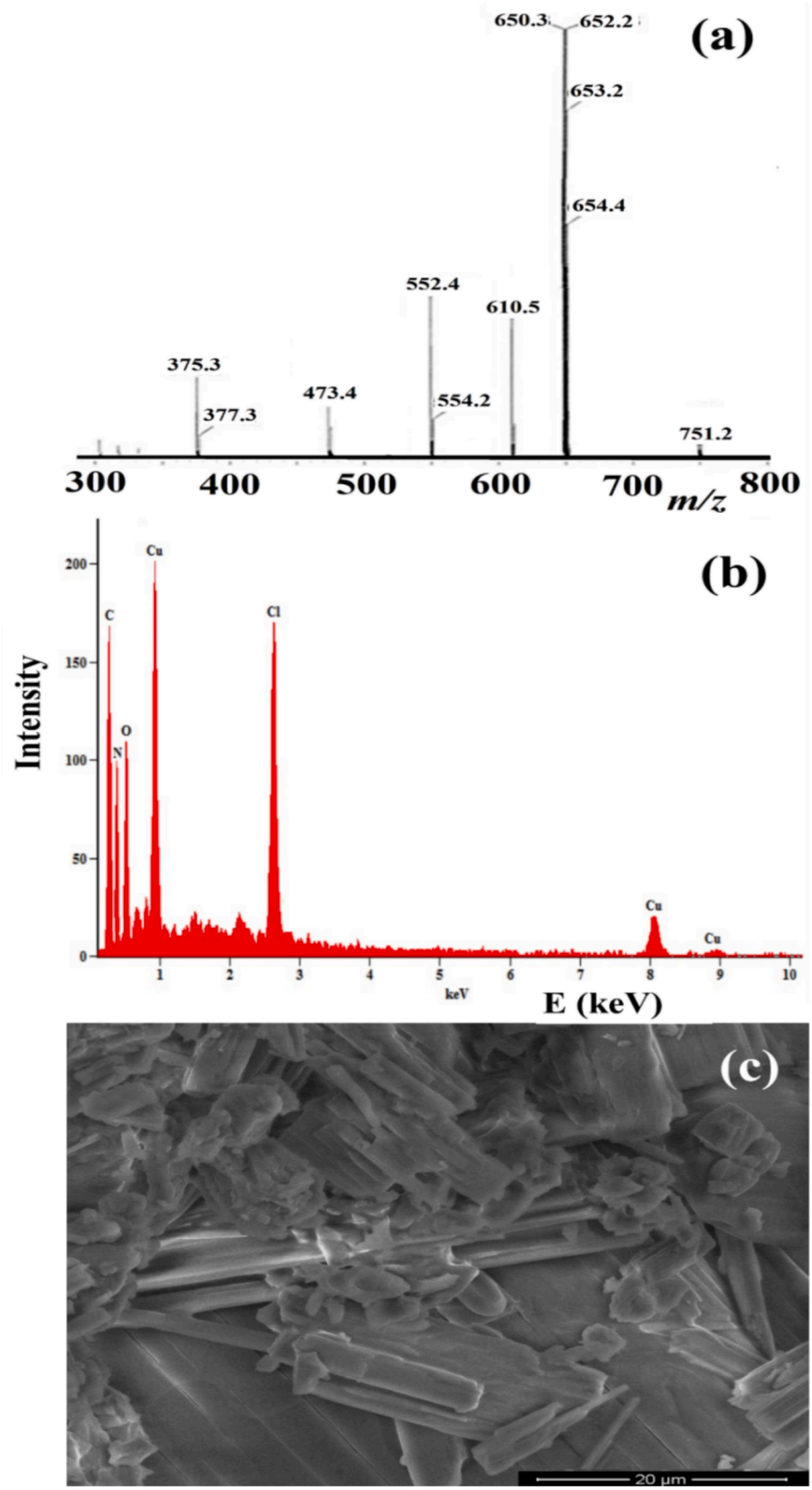

Fig. 1. (a) GC–MS, (b) EDX, and (c) SEM of the *trans*-$(ClO_4)_2Cu^{II}(Me_2N\text{-}Py)_4$ complex.

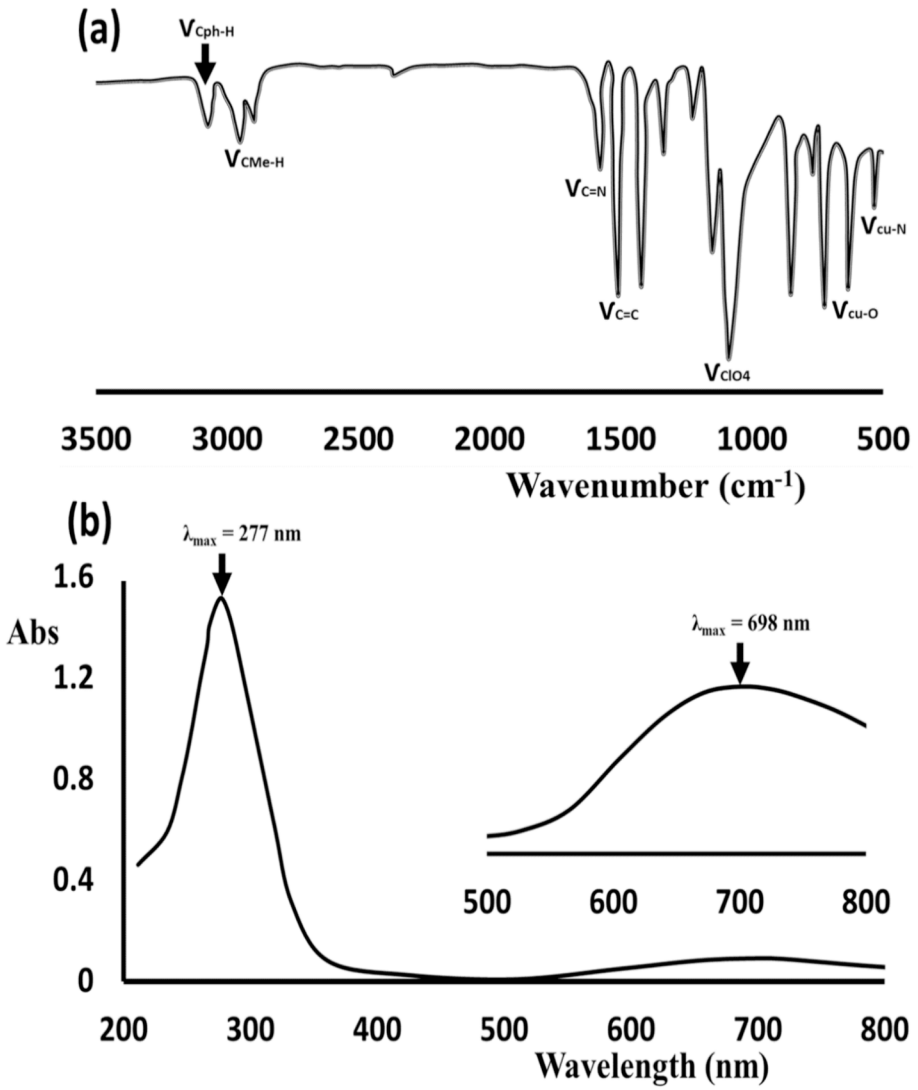

Fig. 2. (a) Solid state FT-IR, and (b) UV–Vis of 1×10^{-4} M of *trans*-$(ClO_4)_2Cu^{II}(Me_2N\text{-}Py)_4$ dissolved in MeOH.

elongation of the Jahn-Teller distortion. The elongation ratio between the average axial and equatorial bonds was found to be approximately 20 %. Moreover, Oh indicated by the sum of the non-classical C_{py}-H…O_{ClO3} and C_{Me}-H…O_{ClO3} H-bond intermolecular forces within the 4 molecules existed in the unit cell as seen in Fig. 3c. Moreover, H-bonds angles of the basal plane measuring 362.27° (Cu1/N3/N4/N5/N6) and 361.68° (Cu2/N1/N2/N13/N10) and the angle subtended by the atoms in the apical position for O1-Cu1-O15A and O14-Cu2-O5B is found to be 168.35° and 158.55°, respectively.

3.3. XRD/HSA-interactions investigation

The presence of ClO_4 anions as multi O contents plays a critical role in building several H-bonds interaction in the *trans*-$(ClO_4)_2Cu^{II}(Me_2N\text{-}Py)_4$ complex lattice as in Fig. 4. The structural analysis revealed that the crystal packing is stabilized by the non-covalent interactions, especially the intermolecular non-classical H-bond interactions. The neighbouring molecules for the symmetry-independent molecule in the asymmetric unit are generated by non-classical C_{py}-H…O and C_{Me}-H…O intermolecular H-bonds (Table 3) resulting in the formation of 2 and 1D-dimensional supramolecular synthons molecular arrangement.

The crystal lattice of *trans*-$(ClO_4)_2Cu^{II}(Me_2N\text{-}Py)_4$ has two primary 2-D synthons. The S9 synthon was produced through non-classical C_{py}–H···$O_{perchlorate}$ and C_{Me}–H···$O_{perchlorate}$ hybrid hydrogen bonds, with bond lengths of 2.652 and 2.550 Å, respectively. In addition, another S6 synthon was formed by combining non-classical C_{Me}–H···$O_{perchlorate}$ and C_{py}–H···$O_{perchlorate}$ with distances of 2.731 and 2.899 Å, respectively (Fig. 4b). In addition, the ClO_4 anions in *trans*-$(ClO_4)_2Cu^{II}(Me_2N\text{-}Py)_4$ also engaged in interactions with adjacent complex molecules. For instance, one of the ClO_4 anions formed a non-classical pure $3C_{Me}$–H···$O_{perchlorate}$ interactions, leading to the formation of 1D-intermolecular interactions all directions among the molecules, resulting an additional lattice stability, as depicted in Fig. 4c.

The HSA is the most effective computational method for clarifying the intermolecular interactions in the XRD-resolved lattice of a certain complex structure (Warad et al., 2019; Al-Zaqri et al., 2020; Warad et al., 2019; Warad et al., 2018; Saleemh et al., 2017; Hema et al., 2020). The 3D-d_{norm} surfaces are graphed using a consistent color scale ranging from −0.3283 to 1.887 range. The examination of *trans*-$(ClO_4)_2Cu^{II}(Me_2N\text{-}Py)_4$ using HSA has verified the presence of multi-distinct red spots within the complex surface, the surface are with 14 spots as depicted in the d_{norm} surface (Fig. 5a). Significantly, the greatest spots are located near the ClO_4 counterions, exhibiting non-classical C_{py}-H….O, and C_{Me}-H….O H-bond short interactions where no other h-bonds like H….N types have been recorded. In addition, the existence of electrophilic hydrogen atoms (blue) and nucleophilic terminal O (red) of the ClO_4 counterions (Fig. 5b) on the molecule surface clarified the creation of these H-bonds. The high H….O contribution ratio of 17.5 % compared

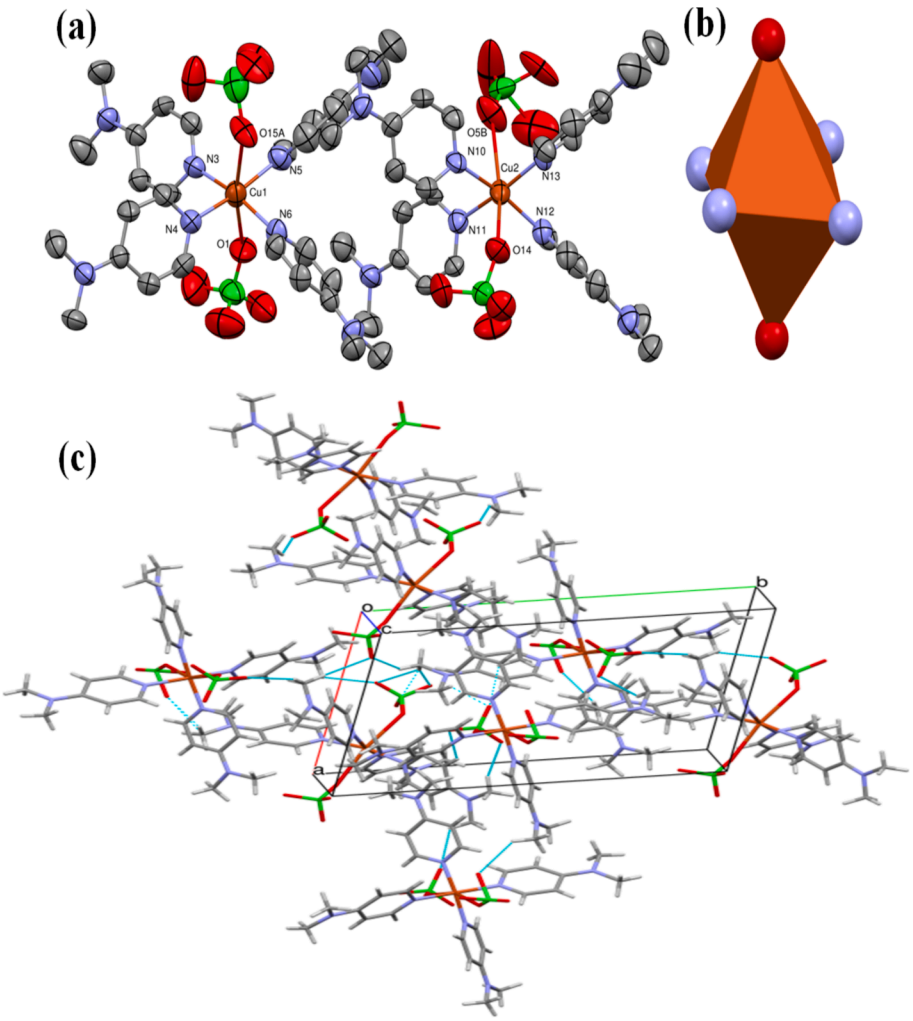

Fig. 3. (a) ORTEP, (b) elongation Jahn-Teller distortion, and (c) 3D-molecular intermoleculars.

Table 2
Selected structure parameters of *trans*-$(ClO_4)_2Cu^{II}(Me_2N\text{-}Py)_4$.

No.	Bond		Å	No.	Angle			(°)
1	Cu01	O007	2.737(6)	1	O007	Cu01	N008	87.2(2)
2	Cu01	N008	2.017(5)	2	O007	Cu01	N009	82.0(2)
3	Cu01	N009	2.012(5)	3	O007	Cu01	N00G	98.7(2)
4	Cu01	N00G	2.008(6)	4	O007	Cu01	N00I	91.0(2)
5	Cu01	N00I	2.015(6)	5	O007	Cu01	O2	176.5(3)
6	Cu01	O2	2.63(1)	6	N008	Cu01	N009	169.0(2)
7	Cl03	O007	1.429(6)	7	N008	Cu01	N00G	90.8(2)
8	Cl03	O00A	1.408(7)	8	N008	Cu01	N00I	89.2(2)
9	Cl03	O00P	1.413(7)	9	N008	Cu01	O2	90.2(3)
10	Cl03	O00R	1.411(6)	10	N009	Cu01	N00G	89.0(2)
11	N008	C00V	1.34(1)	11	N009	Cu01	N00I	92.8(2)
12	N008	C01L	1.324(8)	12	N009	Cu01	O2	100.7(3)
13	N009	C012	1.351(9)	13	N00G	Cu01	N00I	170.3(2)
14	N009	C01A	1.35(1)	14	N00G	Cu01	O2	83.6(3)
15	N00E	C00N	1.35(1)	15	N00I	Cu01	O2	86.7(3)

to the low H….N ratio of 0.8 % supported only the existence of C-H….O nonclassical H-bonds in the complex lattice, the other atom-to-atom (A-to-A) contribution ratios are illustrated in Fig. 5c. The HSA-computational result agreed well with the experimental XRD one.

3.4. TGA analysis

TG-DTG was performed in an open O_2-atmosphere to examine the thermal characteristics of *trans*-$(ClO_4)_2Cu^{II}(Me_2N\text{-}Py)_4$ complex (Fig. 6). The TGA analysis showed that the complex undergoes a mass loss of 65.4 % (Cal, 64.8 %) in the temperature range of 210–395 °C and with T_{DTG} = 260 °C, this step was corresponding to the de-structured or decomposition of the Me_2N-Py organic ligands in the *trans*-$(ClO_4)_2$-$Cu^{II}(Me_2N\text{-}Py)_4$ to light gasses (CO_2 and NO_x) producing the nacked Cu $(ClO_4)_2$ complex. As the temperature increases, the $Cu(ClO_4)_2$ product experiences a further weight reduction of 23.2 % (Cal, 22.9 %) between

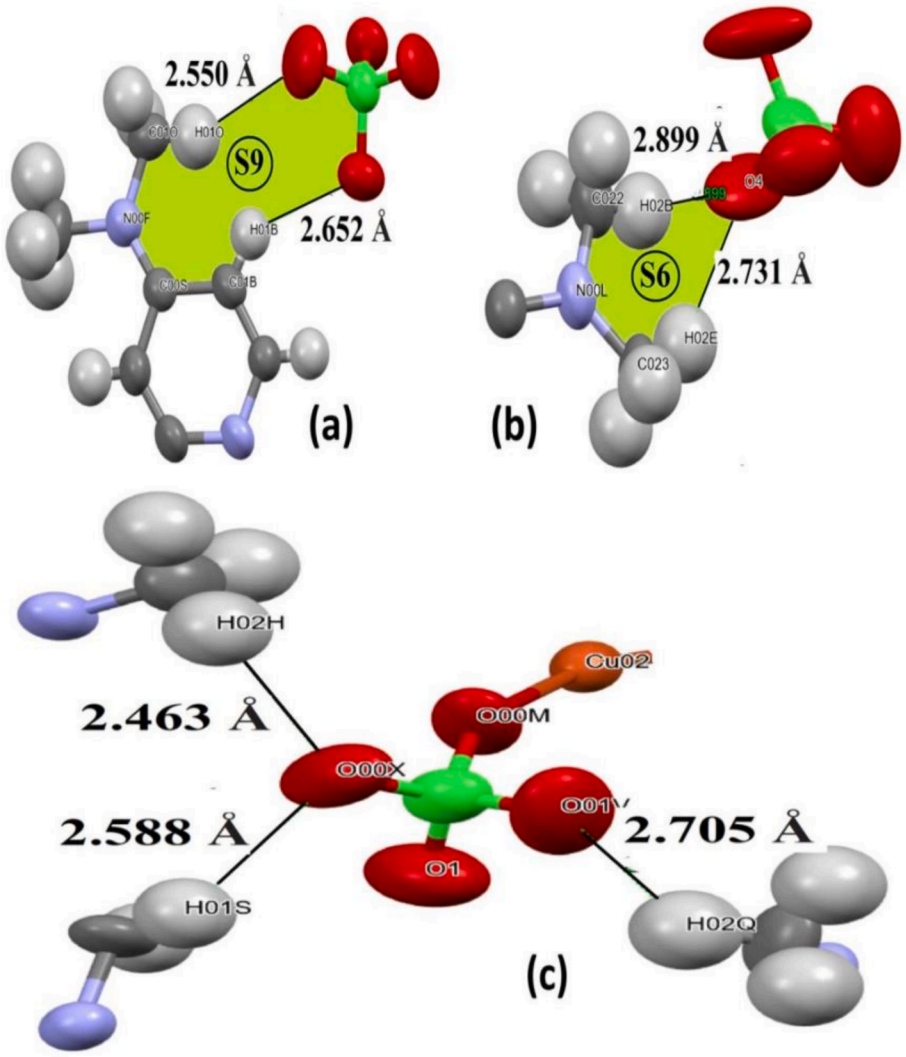

Fig. 4. (a) 2D-S9, (b) 2D-S6 synthons, and (c) 1D-interactions around ClO_4 anion ligand.

Table 3
Total H-bond interactions per *trans*-$(ClO_4)_2Cu^{II}(Me_2N\text{-}Py)_4$ molecule.

D-H…A	D-H (Å)	H…A (Å)	D…A (Å)	D-H…A (°)
C2-H2A…O2	0.96	2.55	3.473(12)	162
C2-H2B…O15	0.96	2.56	3.422(10)	149
C15-H15…O1	0.93	2.55	3.446(19)	161
C20-H20A…O13	0.96	2.55	3.420(12)	151
C36-H36A…O6	0.96	2.45	3.347(13)	155
C33-H36C…O2	0.96	2.53	3.271(12)	135
C15-H15…O1	0.93	2.56	3.056(11)	114
C5-H5…O5	0.93	2.28	3.037(17)	138
C12-H12…O7	0.93	2.55	3.446(19)	161
C34-H34…O13	0.93	2.54	3.313(10)	141
C47-H47…O14	0.93	2.55	3.156(10)	123
C50-H50…O12	0.93	2.48	3.105(13)	125

temperatures of 580–710 °C and with T_{DTG} = 636 °C since ClO_4. The remaining residue corresponding to Cu = O final product (yielding 10.8 %) was proved by FT-IR (Fig. 2a).

3.5. 1BNA DNA docking of trans-$(ClO_4)_2Cu^{II}(Me_2N\text{-}Py)_4$

Molecular docking was used to investigate the electrostatic, hydrophobic, and energetic interactions between *trans*-$(ClO_4)_2Cu^{II}(Me_2N\text{-}Py)_4$ and DNA (PDB:1BNA), since the 1BNA is simple, short and free available. The desired complex occupied the major groove of the 1BNA DNA, and the intricate structure smoothly merged with complex structure volume (Fig. 7a). Significantly, the complex showed binding behaviour similar to the cisplatin complex mode of interaction, as it bonded to both DNA helix through short three hydrogen bonding and one π-π interaction (Fig. 7b). The protons of Pyridine ligands did not show any binding contributions, meanwhile, the protons of Me of dimethyl functional groups played the critical role in the formation of the non-classical H-bonds like DNA:A: DA6:OP2….H-CH_2N with 2.93 Å bond length and DNA:B: DT19:O4….H-CH_2N with 2.88 Å bond length (Fig. 7c) reflecting a positive correlation between the number of formed H-bonds and the binding energy of the complex, which was observed to be −9.45 kcal/mol.

4. Conclusion

A novel *trans*-$(ClO_4)_2Cu^{II}(Me_2N\text{-}Py)_4$ complex was synthesized and investigated utilizing several physicochemical techniques in the current research study. The structural analysis determined that the desire complex exhibited crystalline properties in a triclinic crystal system with the P1 space group. The XRD of Cu(II) ion reflected a distorted Oh geometry, with two perchlorate ions positioned axially and four Me_2N-Py

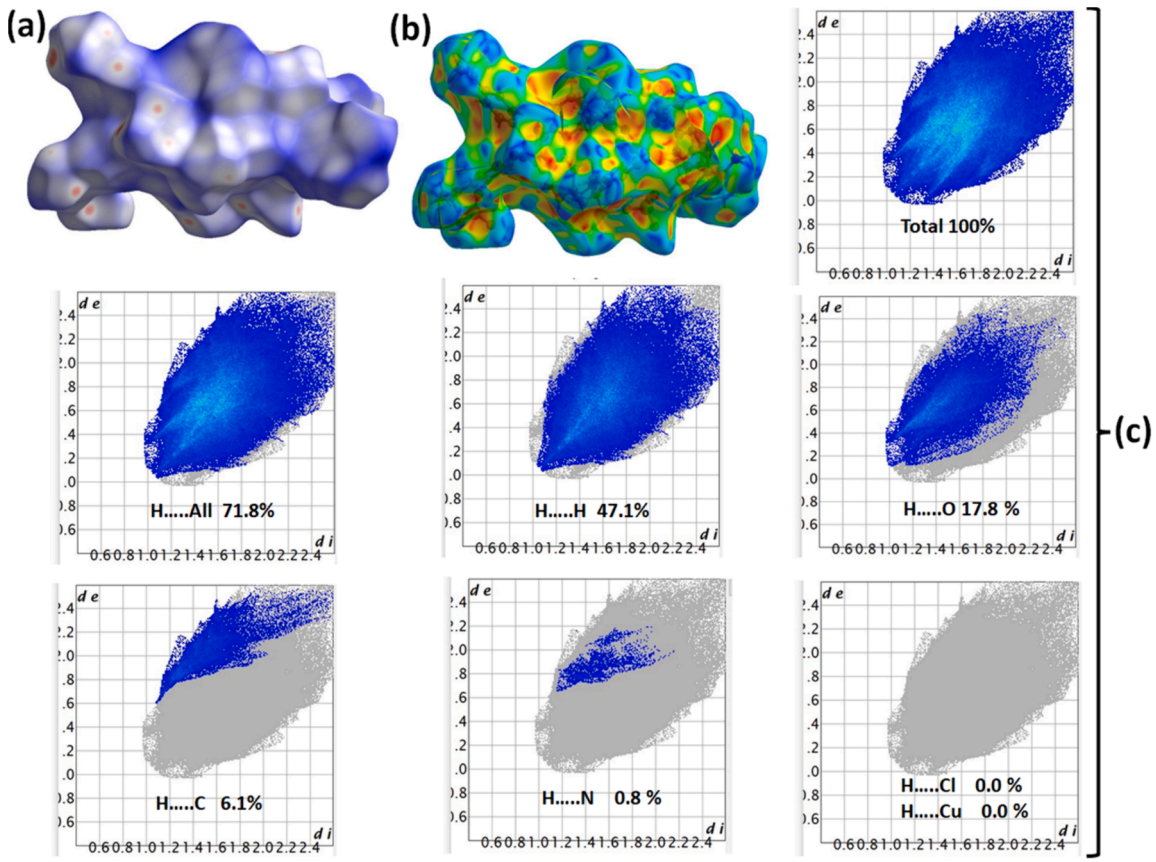

Fig. 5. (a) d_{norm}, (b) shape-index, and (c) A-to-A interactions ratios in *trans*-$(ClO_4)_2Cu^{II}(Me_2N\text{-}Py)_4$.

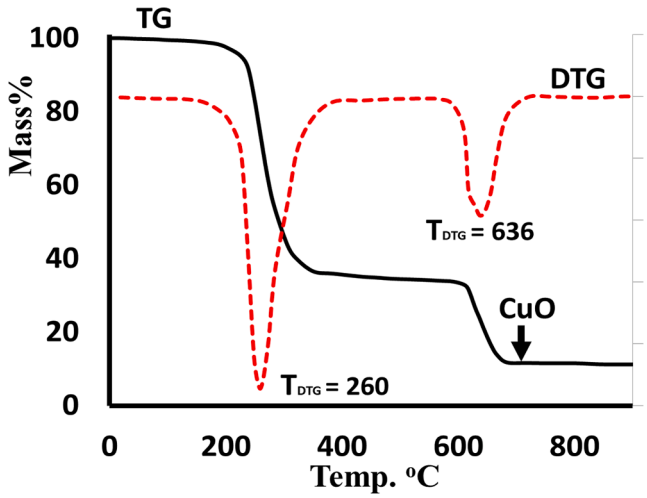

Fig. 6. TG/DTG of *trans*-$(ClO_4)_2Cu^{II}(Me_2N\text{-}Py)_4$ complex.

ligands organized in a planar shape. Additionally, XRD study has shown the presence of a dynamic Jahn-Teller elongation distortion, which has resulted in a 20 % increase in the Cu–O bond lengths. The crystal packing is stabilized by various S9 and S6 synthons intermolecular hydrogen bonding constructed via C_{Me}-H…O and C_{ph}-H…O non-classical interactions. The TG/DTG represented the complex with high thermal stability and two steps degradation mechanism. Furthermore, the docking technique revealed the complex to be a good 1BNA major grove positional binder, showing 2H-bonds and −9.45 kcal/mol binding energy.

CRediT authorship contribution statement

A. AlAli: Writing – original draft, Methodology, Data curation. **A. AlObaid:** Writing – original draft, Methodology, Data curation. **B.S. Chethan:** Methodology, Investigation. **K. Shalalin:** Writing – original draft, Validation, Resources. **N. Alzeqri:** Supervision, Software, Funding acquisition. **K. Alkanad:** Validation, Investigation, Formal analysis. **N. K. Lokanath:** Writing – review & editing, Visualization, Investigation. **A. Zarrouk:** Visualization, Supervision, Data curation. **I. Warad:** Writing – review & editing, Writing – original draft, Supervision, Methodology, Data curation. **S.A. Khanum:** Writing – original draft,

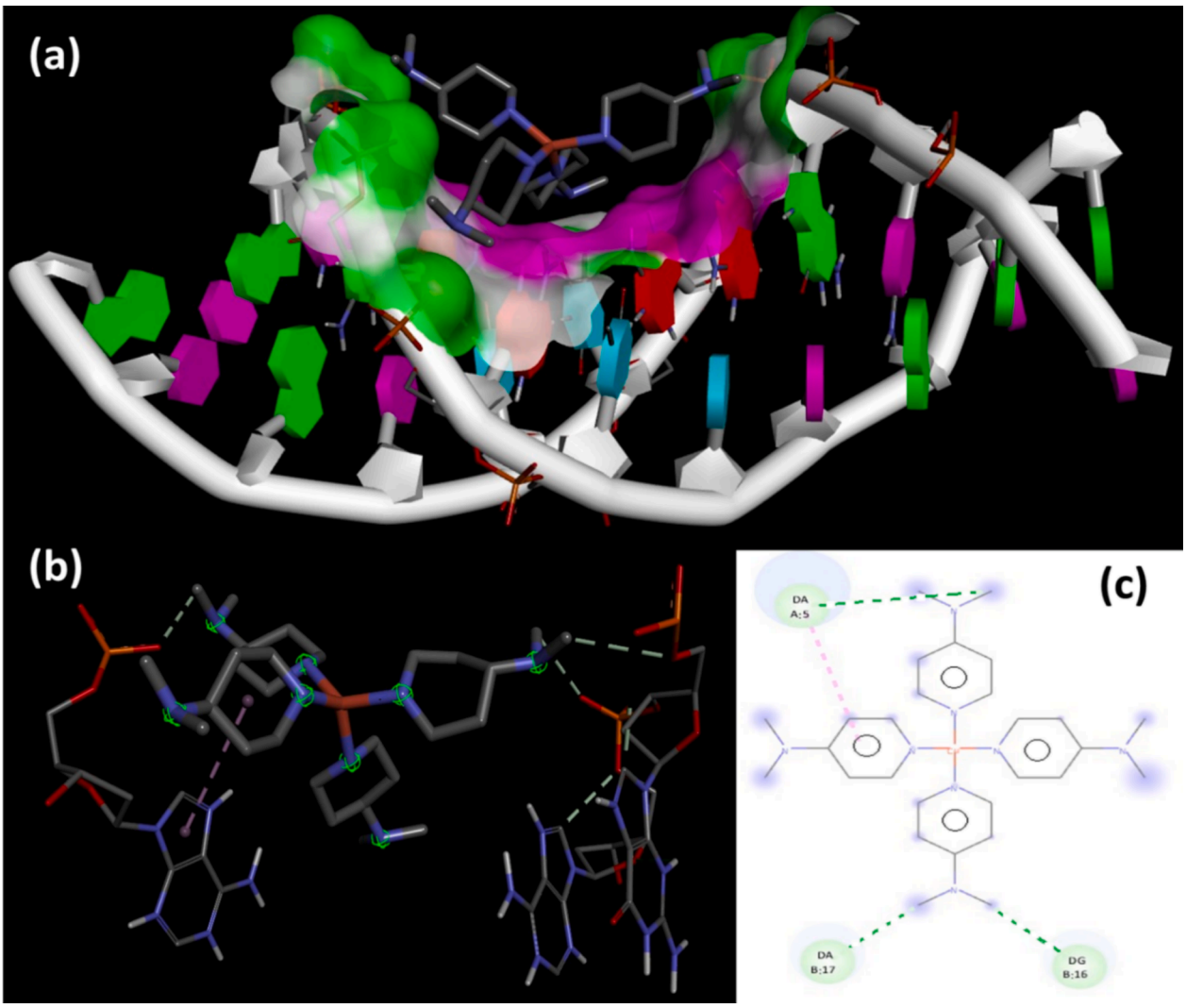

Fig. 7. 1BNA DNA docking, (a) Major groove, (b) cisplatin mode, and (c) 2D-H-bonds interactions.

Software, Resources, Methodology.

Acknowledgements

We extend our appreciation to the Researchers Supporting Project number (RSP2024R381), King Saud University, Riyadh, Saudi Arabia.

Appendix A. Supplementary data

The crystallographic data has been submitted to the Cambridge Crystallographic Data Centre and assigned the additional publication number CCDC **2287195.** To receive copies of this information, you can visit the website www.ccdc.cam.ac.uk/conts/ retrieving.html. Alternatively, you can contact the CCDC at their physical address: 12 Union Road, Cambridge CB2 1EZ, UK. You can also send a fax to +44-1223-336033 or an email to deposit@ccdc.cam.ac.uk. There is no charge for obtaining these copies. Supplementary data to this article can be found online at https://doi.org/10.1016/j.jksus.2024.103302.

References

Adhikari, H.S., Garai, A., Manandhar, K.D., Yadav, P.N., 2022. Pyridine-based NNS tridentate chitosan thiosemicarbazones and their copper(II) complexes: Synthesis, characterization, and anticancer activity. ACS Omega 7, 30978. https://doi.org/10.1021/acsomega.2c02966.

A. AlAli, M. Al-Noaimi, A. AlObaid, H. A. Khamees, A. Zarrouk, K. Kumara, I. Warad, S. A. Khanum, Jahn-Teller distortion in SP-like [Cu(bipy)(triamine)].2BF_4 complexes with novel NH… F/CH… F synthon: XRD/HSA-interactions, physicochemical, electrochemical, DFT, docking and COX/LOX inhibition, J. Mol. Liq. 387 (2023) 122689. doi: 10.1016/j.mol liq.2023.122689.

AlAli, A., Khamees, H.A., Madegowda, M., Zarrouk, A., Kumara, K., El-khatatneh, N., Warad, I., Khanum, S.A., 2023. One-pot reproducible Sonosynthesis of trans-[Br(N∩N')Cu(μBr)$_2$Cu(N∩N')Br] dimer:[H….Br S(9)] synthons, spectral, DFT/XRD/HSA, thermal, docking and novel LOX/COX enzyme inhibition. J. Mol. Struct. 1275, 134626 https://doi.org/10.1016/j.molstruc.2022.134626.

Alem, M.B., Desalegn, T., Damena, T., Bayle, E.A., Koobotse, M.O., Ngwira, K.J., Ombito, J.O., Zachariah, M., Demissie, T.B., 2023. Cytotoxicity and antibacterial potentials of mixed ligand Cu(II) and Zn(II) complexes: a combined experimental and computational study. ACS Omega 8, 13421. https://doi.org/10.1021/acsomega.3c00916.

Al-Zaqri, N., Salih, K.S.M., Awwadi, F.F., Alsalme, A., Alharthi, F.A., Alsyahi, A., Al Ali, A., Zarrouk, A., Aljohani, M., Chetouni, A., Warad, I., 2020. Synthesis, physicochemical, thermal, and XRD/HSA interactions of mixed [Cu(Bipy)(Dipn)](X) 2 complexes: DNA binding and molecular docking evaluation. J. Coord. Chem. 73, 3236. https://doi.org/10.1080/00958972.2020.1841898.

Andrejević, T.P., Aleksic, I., Kljun, J., Počkaj, M., Zlatar, M., Vojnovic, S., Nikodinovic-Runic, J., Turel, I., Djuran, M.I., Glišić, B.D., 2023. Copper (II) and silver (I) complexes with dimethyl 6-(pyrazine-2-yl) pyridine-3, 4-dicarboxylate (py-2pz): the influence of the metal ion on the antimicrobial potential of the complex. RSC Adv. 13, 4376. https://doi.org/10.1039/d2ra07401j.

Anupama, B., Aruna, A., Manga, V., Sivan, S., Sagar, M.V., Chandrashekar, R., 2017. Synthesis, spectral characterization, DNA/protein binding, DNA cleavage, cytotoxicity, antioxidative and molecular docking studies of Cu (II) complexes containing Schiff base-bpy/phen ligands. J. Fluoresc. 27, 953.

Balakrishnan, C., Theetharappan, M., Kowsalya, P., Natarajan, S., Neelakantan, M.A., Mariappan, S.S., 2017. Biocatalysis, DNA–protein interactions, cytotoxicity and

molecular docking of Cu (II), Ni(II), Zn(II) and V(IV) Schiff base complexes. Appl. Organomet. Chem. 31, 3776. https://doi.org/10.1002/aoc.3776.
Begum, A.B., Rekha, N.D., Vasantha Kumar, B.C., Lakshmi Ranganatha, V., Khanum, S. A., 2014. Synthesis, characterization, biological and catalytic applications of transition metal complexes derived from Schiff base. Bioorg. Med. Chem. Lett. 24, 3559. https://doi.org/10.1016/j.bmcl.2014.05.046.
Czaikowski, M.E., McNeece, A.J., Boyn, J.N., Jesse, K.A., Anferov, S.W., Filatov, A.S., Mazziotti, D.A., Anderson, J.S., 2022. Generation and aerobic oxidative catalysis of a Cu (II) superoxo complex supported by a redox-active ligand. J. Am. Chem. Soc. 144, 15569. https://doi.org/10.1021/jacs.2c04630.
Fathima, S.S.A., Meeran, M.M.S., Nagarajan, E.R., 2020. Synthesis, characterization and biological evaluation of novel 2, 2′-((1, 2-diphenylethane-1,2-diylidene)bis(azanylylidene)) bis (pyridin-3-ol) and metal complexes: molecular docking and in silico ADMET profile. Struct. Chem. 31, 521. https://doi.org/10.1007/s11224-019-01425-7.
Fathy, A.M., Hessien, M.M., Ibrahim, M.M., Ramadan, A.E., 2022. Anionic ligands tune the structural and catalytic properties of quinoxaline-based copper (II) complexes as mimetics of copper-containing oxidase protein. J. Mol. Struct. 1250, 131809 https://doi.org/10.1016/j.molstruc.2021.131809.
Fu, X.B., Zhang, J.J., Liu, D.D., Gan, Q., Gao, H.W., Mao, Z.W., Le, X.Y., 2015. Cu (II)–dipeptide complexes of 2-(4′-thiazolyl) benzimidazole: Synthesis, DNA oxidative damage, antioxidant and in vitro antitumor activity. J. Inorg. Biochem. 143, 77. https://doi.org/10.1016/j.jinorgbio.2014.12.006.
Graur, V., Usataia, I., Graur, I., Garbuz, O., Bourosh, P., Kravtsov, V., Lozan-Tirsu, C., Balan, G., Fala, V., Gulea, A., 2023. Novel copper(II) complexes with N 4, S-diallylisothiosemicarbazones as potential antibacterial/anticancer drugs. Inorg. 11, 195. https://doi.org/10.3390/inorganics11050195.
Handy, J.V., Ayala, G., Pike, R.D., 2017. Structural comparison of copper (II) thiocyanate pyridine complexes. Inorg. Chim. Acta. 456, 64. https://doi.org/10.1016/j.ica.2016.11.013.
Haynes, J.S., Rettig, S.J., Sams, J.R., Thompson, R.C., Trotter, J., 1987. Structure and magnetic exchange in poly-bis (pyrazine) bis (methanesulfonato-o)-copper (II). One-dimensional exchange in a two-dimensional polymer. Can. J. Chem. 65, 420. https://doi.org/10.1139/v87-071.
Hema, K., Warad, I., Karthik, S., Zarrouk, A., Kumara, K., Pampa, J., Mallu, P., Lokanath, K., 2020. XRD/DFT/HSA-interactions in Cu(II)Cl/phen/ß-diketonato complex: physicochemical, solvatochromism, thermal and DNA-binding analysis. J. Mol. Struct. 1210, 128000 https://doi.org/10.1016/j.molstruc.2020.128000.
Jevtovic, V., Alshamari, A.K., Milenković, D., Dimitrić Marković, J., Marković, Z., Dimić, D., 2023. The effect of metal ions (Fe Co, Ni, and Cu) on the molecular-structural, protein binding, and cytotoxic properties of metal pyridoxal-thiosemicarbazone complexes. Int. J. Mol. Sci. 24, 11910. https://doi.org/10.3390/ijms241511910.
Jiang, D., Men, L., Wang, J., Zhang, Y., Chickenyen, S., Wang, Y., Zhou, F., 2007. Redox reactions of copper complexes formed with different β-amyloid peptides and their neuropathalogical relevance. Biochem. 46, 9270. https://doi.org/10.1021/bi700508n.
Kongchoo, S., Kantacha, A., Saithong, S., Wongnawa, S., 2016. Synthesis, crystal structure, and spectroscopic properties of Cu (II) complex with 14-membered hexaazamacrocyclic ligands. J. Chem. Crystallogr. 46, 222. https://doi.org/10.1007/s10870-016-0649-8.
Masternak, J., Zienkiewicz-Machnik, M., Łakomska, I., Hodorowicz, M., Kazimierczuk, K., Nosek, M., Majkowska-Młynarczyk, A., Wietrzyk, J., Barszcz, B., 2021. Synthesis and structure of novel copper (II) complexes with N, O-or N, N-donors as radical scavengers and a functional model of the active sites in metalloenzymes. Int. J. Mol. Sci. 22, 7286. https://doi.org/10.3390/ijms22147286.
Nnabuike, G.G., Salunke-Gawali, S., Patil, A.S., Butcher, R.J., Obaleye, J.A., Ashtekar, H., Prakash, B., 2023. Copper (II) complexes containing derivative of aminobenzoic acid and nitrogen-rich ligands: synthesis, characterization and cytotoxic potential. J. Mol. Struct. 1279, 135002 https://doi.org/10.1016/j.molstruc.2023.135002.
Patel, R.N., Shukla, K.K., Singh, A., Choudhary, M., Patel, D.K., 2010. Synthesis, characterization, crystal structures, and superoxide dismutase activity of copper (II) octahedral complexes containing tri-and monodentate ligands. J. Coord. Chem. 63, 586. https://doi.org/10.1080/0095897 1003628850.
Puchoňová, M., Švorec, J., Švorc, L., Pavlik, J., Mazúr, M., Dlháň, L., Růžičková, Z., Moncoľ, J., Valigura, D., 2017. Synthesis, spectral, magnetic properties, electrochemical evaluation and SOD mimetic activity of four mixed-ligand Cu (II) complexes. Inorga. Chim. Acta 455, 298. https://doi.org/10.1016/j.ica.2016.10.034.
Saleemh, F.A., Musameh, S., Sawafta, A., Brandao, P., Tavares, C.J., Fer-dov, S., Barakat, A., Al Ali, A., Al-Noaimi, M., Warad, I., 2017. Diethylenetri-amine/diamines/copper(II) complexes [Cu(dien)-(NN)]Br 2: Synthesis, solvatochromism, thermal, electrochemistry, single crystal, Hirshfeld surface analysis and antibacterial activity. Arab. J. Chem 10, 845. https://doi.org/10.1016/j.arabjc.2016.10.008.
Santana, F.S., Briganti, M., Cassaro, R.A.A., Totti, F., Ribeiro, R.R., Hughes, D.L., Nunes, G.G., Reis, D.M., 2020. An oxalate-bridged copper (II) complex combining monodentate benzoate, 2, 2′-bipyridine and aqua ligands: synthesis, crystal structure and investigation of magnetic properties. Molecules 25, 1898. https://doi.org/10.3390/molecules25081898.
G.M. Sheldrick, A short history of SHELX, Acta Crystallogr., Sect A64 (2008) 112. doi: 10.1107/S0108767307043930.
E. Spodine, J. Manzur, M. T. Garland, J. P. Fackler Jr, R. J. Staples, and B. Trzcinska-Bancroft, Copper complexes with di-pyridylmethane. The synthesis and X-ray structures of bis (di-pyridylmethane) copper (I) perchlorate, bis (di-pyridylmethane) copper (II) perchlorate and dichloro-μ-dichloro-bis (di-pyridylmethane) dicopper (II), Inorg. Chim. Acta. 203 (1993) 73. doi: 10.1016/S0020-1693(00)82907-2.
Warad, I., Awwadi, F.F., Daqqa, M., Al Ali, A., Ababneh, T.S., AlShboul, T.M., Jazzazi, T. M., Al-Rimawi, F., Hadda, T.H., Mabkhot, Y.N., 2017. New isomeric Cu (NO_2-phen) 2Br] Br complexes: crystal structure, Hirschfeld surface, physicochemical, solvatochromism, thermal, computational and DNA-binding analysis. J. Photochem. Photobiol. b, Biol. 171, 9. https://doi.org/10.1016/j.jphotobiol.2017.04.017.
Warad, I., Abdoh, M., Al Ali, A., Shivalingegowda, N., Kumara, K., Zarrouk, A., Lokanath, N.K., 2018. Synthesis, spectra and X-ray crystallography of dipyridin-2-ylmethanone oxime and its CuX_2(oxime)$_2$ complexes: thermal, Hirshfeld surface and DFT analysis. J. Mol. Struct. 1154, 619. https://doi.org/10.1016/j.molstruc.2017.10.087.
Warad, I., Awwadi, F.F., Abd Al-Ghani, B., Sawafta, A., Shivalingegowda, N., Lokanath, N.K., Mubarak, M.S., Ben Hadda, T., Zarrouk, A., Al-Rimawi, F., Odeh, A. B., Barghouthi, S.A., 2018. Ultrasound-assisted synthesis of two novel [CuBr (diamine)$_2$.H_2O] Br complexes: solvatochromism, crystal structure, physicochemical, Hirshfeld surface thermal, DNA/binding, antitumor and antibacterial activities. Ultrason. Sonochem. 48, 1. https://doi.org/10.1016/j.ultsonch.2018.05.009.
Warad, I., Alkanad, K., Suleiman, M., Kumara, K., Al-Ali, A., Mohammed, Y.H., Lokanath, N.K., Zarrouk, A., 2019. Design, structural, C-H…. H–C supramolecular interactions and computational investigations of Cd (N∩ N ″) X2 complexes based on an asymmetrical 1, 2-diamine ligand: physicochemical and thermal analysis. J. Coord. Chem. 72, 3285. https://doi.org/10.1080/00958972.2019.1696960.
Warad, I., Musameh, S., Sawafta, A., Brandão, P., Tavares, C.J., Zarrouk, A., Amereih, S., Al Ali, A., Shariah, R., 2019. Ultrasonic synthesis of Oct. *trans*-Br 2Cu(N∩N)2 Jahn-Teller distortion complex: XRD-properties, solvatochromism, thermal, kinetic and DNA-binding evaluations. Ultrason. Sonochem. 52, 428. https://doi.org/10.1016/j.ultsonch.2018.12.019.
Wolff, S.K., Grimwood, D.J., McKinnon, J.J., Jayatilaka, D., Spackman, M.A., 2007. Crystal explorer 2.1. University of Western Australia, Perth.
Zabiulla, S., Kouser, M.J., Begum, A.B., Asha, M.S., Al-Ostoot, F.H., Lakshmeesha, D.P., Ramu, R., Khanum, S.A., 2023. Molecular docking, synthesis and antimicrobial evaluation of metal complexes with schiff base. Results Chem. 5, 100650 https://doi.org/10.1016/j.rechem.2022.100650.
Zeisel, L., Szimhardt, N., Wurzenberger, M.H.H., Klapötke, T.M., Stierstorfer, J., 2019. 2-Methylsubstituted monotetrazoles in copper(II) perchlorate complexes: manipulating coordination chemistry and derived energetic properties. New J. Chem. 43, 609. https://doi.org/10.1039/C8NJ05375H.